Possible Near-II? Channels for Remote Sensing **Precipitable** Water **Vapor** from **Geostationary** Satellite Platforms

B.-C. GAO*

Center for the Study of Earth from Space/CIRES, University of Colorado, Boulder, Colorado

A, F. H. GOETZ

Center for the Study of Earth from Space/CIRES, and Department of Geological Sciences, University of Colorado, Boulder, Colorado

ED R. WESTWATER

NOAA/ERL/Wave Propagation Laboratory, Boulder, Colorado

J. E. CONEL AND R. O. GREEN

Jet Propulsion Laboratory, Pasadena, California

(Manuscript received 20 July 1992, in final form 26 January 1993)

ABSTRACT

Remote sensing of tropospheric water vapor profiles from *current* geostationary writher satellites are made using a few broadband infrared (IR) channels in the 6–13-μm region. Uncertainties greater than 20% exist in derived water vapor values just above the surface from the IR emission measurements. [n this paper, we propose three near-IR channels. one within the 0.94-μm water vapor band absorption region. and the other two in nearby atmospheric **windows. for remote** sensing of precipitable water vapor over land areas. excluding lakes and rivers, during daytime from future geostationary satellite platforms. **The** physical principles are as follows. **The reflectance of most surface targets vanes approximately linearly with wavelength near I μm. The solar radiation on the sun–surface–sensor ray path is attenuated by atmospheric water vapor. The ratio of the radiance from the absorption channel with the radiances from the two window channels removes the surface reflectance** effects and **yields approximately the mean atmospheric water vapor** transmittance of **the absorption channel. The integrated** water vapor **amount from ground to space can be obtained with a precision of better than 5% from the mean transmittance. Because surface** reflectances vary slowly **with** time. temporal **variation** of precipitable water vapor can **be** determined **reliably.** High spatial resoluti **cm.** precipitable **water** vapor images **are derived** from **spectral** data **collected** by the Airborne *Visible-Inl'rared* Imaging Spectrometer, which measures **solar** radiation reflected by **the** surface in the 0.4–2.5-μm region in 10-nm **channels** and has a **ground** instantaneous field of view of 20 **m from** its **platform on** an ER-2 aircraft at 20 **km. 1 he proposed** near-IR reflectance **technique would complement the** IR emission techniques **for** remote sensing of water vapor profiles **from** geostatio **nary** satellite **platforms,** especially in **the boundary** layer **where** most of **the** water vapor is located.

1. Introduction

Tropospheric water vapor is quite variable both temporally and spatially. Frequent measurements of water vapor vertical profiles at good vertical and horizontal resolution over large geographical areas are useful for meteorological applications. The geostationary satellite platforms are most suitable for frequent measurements with large area coverages. In this paper, the integrated water vapor content from ground to space is refereed to as the column water vapor amount, or as the precipitable water vapor.

Present satellite capabilities in remote sensing of water vapor have been summarized by Starr and Melfi (199 I). The Visible-Infrared Spin Scan Radiometer (VISSR) Atmospheric Sounder (VAS) on the current Geostationary Operational Environmental Satellite (GOES) typically provides data at a temporal resolution of approximately 90 min and with a spatial resolution of approximately 30 km, and was originally designed mainly for remote sensing of atmospheric temperature profiles (Rao et al. 1990). However, a few broadband channels in the 6- 13-gin region also have sensitivity to water vapor, and a split window technique (Chesters et al. 1983) has been used in deriving moisture fields. Since 1987 a physically based technique

" Current affiliation: University Space Research Association, Code 913, NASA/Goddard Space flight Center, Greenbelt, MD 20770.
Corresponding author address: Dr. Bo-Cai Gao, NASA /Goddard Space Flight Center, Code 913, Greenbelt, MD 20771.

DE

(Hayden 1988) has been used for operational retrievals of both temperature and water vapor profiles at coarse vertical resolution. The results show clearly the capability for observing large-scale temperature and moisture structures. The main weaknesses are the bias errors in the retrievals, the dependence on the first guesses, and the effects of clouds. So far, limited quantitative information on water vapor distribution has been derived from GOES VAS measurements (Starr and Melfi 1991).

The current operational infrared-microwave sounding system (TOVS) on polar-orbiting platforms was designed for remote sensing of temperature and water vapor profiles at a temporal resolution of approximately six hours. The High-Resolution Infrared Sounder (HIRS-2) of TOVS has nearly twice as many channels as VAS. Water vapor profiles have been derived from measurements in five broadband infrared channels between 6 and 14 pm. These channels also have temperature sensitivity, A physically based technique (Susskind et al. 1984) has been developed for retrieving temperature and water vapor profiles from TOVS measurements. The uncertainty of the retrieved column water vapor amount is approximately ±20%. The uncertainties of water vapor vertical profiles at different pressure levels are larger than 20% (Starr and Melfi 1991). Although HIRS-2 has more channels than VAS. the retrieved water vapor profiles also show dependence on the first-guess temperature and water vapor profiles, with the greatest dependence close to the surface (Reuter et al. 1988).

The next generation of geostationary weather satellites (GOES I-M series) (Rao et al. 1990) will have improved imaging and sounding systems. The sounding systems will have 18 [R channels. similar to those of HIRS-2. for remote sensing of temperature and water vapor profiles. Therefore, the capability of remote sensing of water vapor profiles from GOES I-M series satellites is expected to be comparable to that of the current HIRS-2.

In this paper, we discuss the possibility of remote sensing of column water vapor, mostly located in the boundary layer of the atmosphere, from measurements of solar radiation near 1 μm reflected by land surfaces from geostationary satellite platforms.

2. Remote sensing of water vapor using the 0.94-pm band

Remote sensing of atmospheric water vapor from the ground has been achieved by measuring transmitted solar radiation in two near-i R channels (Fowle 1912: Voltz 1974; Bird and Hustrom 1982). One channel is within the 0.94-μm water vapor absorption band, and the other is a window channel near 0.86 μm. The ratio of the radiance from the absorption channel with the radiance from the window channel equals the mean atmospheric water vapor transmittance multiplied by a constant. The constant is equal to the ratio of the exoatmospheric solar irradiance at the absorption channel to that at the window channel. The amount of water vapor is derived from the transmittance.

Remote sensing of water vapor from an aircraft platform has been made from measurements of solar radiation near 1 μm reflected by land surface targets (Ciao and Goetz 1990; Frouin et al. 1990). Column water vapor with a precision of better than 5% has been obtained (Gao and Goetz 1990) from airborne imaging spectrometer data by curve fitting observed spectra with calculated spectra in the 0.94- and the 1. 14-μm water vapor band absorption regions using a nonlinear least-squares fitting technique. During the fitting process the surface reflectance are assumed to vary linearly with wavelength in the two water vapor band absorption regions. A recent comparison (Gao et al, 1992) of water vapor retrievals from airborne imaging spectrometer data using the curve fitting technique and water vapor retrievals from ground-based upward-looking microwave emission measurements has shown that the results from the two kinds of measurements agree to O. I cm when the atmospheric column water vapor amount is approximately 0.7 cm.

Column water vapor has been derived using the so-called "differential absorption technique" (Frouin et al. 1990). In this technique, the solar radiation reflected by the earth's surface is measured in two near-IR channels centered at the same wavelength of O.935 μm but with different widths. The width of the narrow channel is 17 nrn, and that of the broad channel 45 nm. The two channels have different sensitivities to water vapor changes. especially when the amount of water vapor in the atmosphere is small. The ratio of radiances from the two channels is nearly independent of surface reflectances. A test of the technique using data measured from a low-flying aircraft platform gives column water vapor amount with a precision of approximately 15%. The lower precision of this technique, relative to that of the curve fitting technique, is due to the fact that both the narrow and the broad channels have sensitivities to water vapor changes and the two-channel ratio is therefore less sensitive to water vapor changes.

3. Selection of near-IR channels for geostationary satellites

The curve fitting technique for deriving column water vapor requires measurements of reflected solar radiation at high spectral resolution so that the shape of the water vapor band can be resolved. This, in turn. requires spectral measurements in approximately 20 channels at 10-nm resolution, to cover the whole 0.94-μm water vapor absorption region and nearby atmospheric window regions. It is not practically feasible in the near future to add this many near-IR channels to a geostationary weather satellite for measuring column water vapor amounts.

For column water vapor amounts of at least 4 cm, the radiance from the 17-rim narrow channel used in the differential absorption technique of Frouin et al. (1990) is very small because of the saturated water vapor absorption, The saturation effect is further discussed in section 3b. If the widths of both narrow and broad channels are increased, the differential sensitivity to water vapor, and therefore retrieval sensitivity, is lost. Therefore, the differential absorption technique of Frouin et al. (I 990) is not appropriate for remote sensing water vapor from geostationary satellite platforms.

We propose the use of three near-IR channels, one within the 0.94-pm water vapor band absorption region, and the other two in nearby atmospheric windows, for remote sensing water vapor over land areas from future geostationary satellite platforms. The technique of remote sensing water vapor from space described in this paper is referred to as the "reflectance technique." The reasons for making this choice, that is. one absorption channel and two window channels, will become clear later. In order to properly select the positions and widths of the three near-IR channels, the absorption and scattering properties of the atmospheric gases and aerosols, the channel sensitivities to water vapor, the surface reflectance properties, and the long-term variations in spectral responses of satellite instruments must be taken into consideration,

a) Absorption and scattering properties near 1 μm

1 he radiance at a downward-looking satellite sensor can be written (Esaias et al. 1986) in a simplified form as

$$L_{sensor}(\lambda) = L_{sun}(\lambda)T(\lambda)R(\lambda) + L_{path}(\lambda) \quad (1)$$

where λ is the wavelength, $L_{sensor}(\lambda)$ is the radiance at the sensor. L_{sun} is the solar radiance above the atmosphere, $T(\lambda)$ is the total atmospheric transmittance, which is equal to the product of the atmospheric transmittance from the sun to the earth's surface and that from the surface to the satellite sensor, $R(\lambda)$ is the surface bidirectional reflectance, and L@(A) is the path-scattered radiance. The first term on the right side of Eq. (I) is the direct reflected solar radiation; L_{direct} is used to represent this component; $L_{sensor}(\lambda)/L_{sun}(\lambda)$ is defined as the apparent reflectance $R^*(\lambda)$ in this paper.

The 7'(A) contains information about the total amount of water vapor in the combined sun-surface sensor path: $L_{sun}(\lambda)$ is a known quantity. Near I μm, Rayleigh scattering is negligible and the main contribution to $L_{path}(\lambda)$ is scattering by aerosols; $L_{path}(\lambda)$ in the 1-μm region is usually about 10% of the direct reflected solar radiation. Because most aerosols are located in the lower 2 km of the atmosphere and the same is true for atmospheric water vapor molecules, the single and multiple scattered radiation by aerosols is also subjected to water vapor absorption. As a result, $L_{path}(\lambda)$ contains water vapor absorption features (Gao and Goetz 1990). We assume that $L_{path}(\lambda)$ can be treated approximately as a fraction of direct reflected solar radiation when the aerosol concentrations are low. This assumption allows the derivation of column water vapor amounts from satellite data without the need of modeling single and multiple scattering effects.

b) Sensitivity of the O.94-μm water vapor band

According to Iqbal (1983), the monthly means of column water vapor in different parts of the United States are typically in the range 0.5-4.3 cm. Figure I shows the calculated total atmospheric gaseous transmittance spectra in a sun-surface-sensor ray path for column water vapor amounts of O.6, 1.2, 2.5, and 5.0 cm in the 0.8-1. I -μm region. The calculations were for a solar zenith angle of 60° and for an observational zenith angle of 45°, The two angles are relative to the local vertical direction of the surface pixel (the ground instantaneous field of view) being viewed. The calculations used the midlatitude summer atmospheric model of LOWTRAN-6 (Kneizys et al. 1983) with the total amount of water vapor in the model being scaled by appropriate factors. The calculations used the Malkmus (1967) narrowband spectral model with the

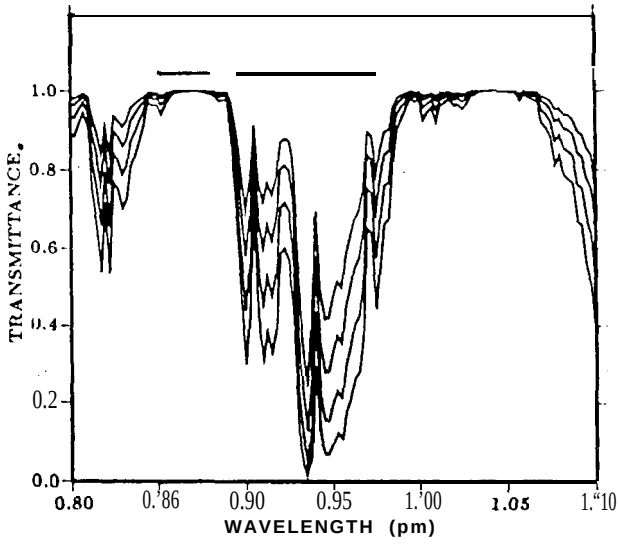

FIG. 1. Calculated atmospheric gaseous transmittance spectra in the 0.8-1.1-μm region for a sun-surface-satellite ray path at different water vapor amounts, 'f he four curves from the top to the bottom correspond to column water vapor amounts of 0.6, 1.2.2.5. and 5.0 *cm. respectively.* The calculations were made for a solar zenith angle of 60° and an observational zenith angle of 4S°. The calculations used the midlatitude summer model of LOWTRAN-6 (Kneizys et al. 1983) with the total amount of water vapor in the model being scaled by appropriate factors, The bandpasses of the proposed two window channels centered at 0.865 and 1.04 μm and one *water* vapor absorption channel centered at 0.935 μm are marked with thick her. izontal lines.

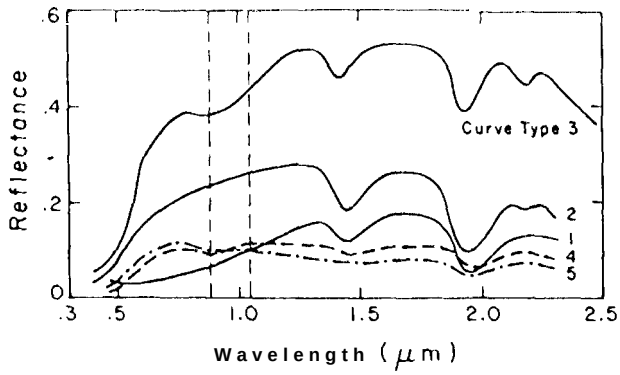

FIG. 2. Typical soil reflectance curves for five major soil types (Condit 1970; Stoner and Baumgartner 1980): (1) organic dominated, moderately fine texture; (2) organic affected, moderately course texture; (3) iron dominated laterite-type soil; (4, 5) iron- and organic-rich soil, respectively. The vertical dashed lines represent the 0.94-μm water vapor band region.

model parameters having a spacing of 2.5 nm. The two narrow regions around 0.865 and 1.04 μm have little gaseous absorption; these regions are often referred to as the atmospheric windows. In the absorption region between approximately 0.89 and 1.0 μm, the absorption vanes significantly. The strongest absorption occurs at 0.935 μm. As the column water vapor amount increases from 2.5 to 5.0 cm, there is little change in the peak absorption at 0.935 μm. This is the saturation effect mentioned previously. At wavelengths near 0.90 and 0.98 μm, the absorption is much weaker than that at 0.935 pm. Numerical calculations show that the strong absorption region around 0.935 μm has the greatest sensitivity to water vapor changes for conditions of column water vapor amounts less than approximately 1 cm (Kaufman and Gao 1990), while the weaker absorption regions around 0.90 and 0.98 μm are more sensitive to water vapor changes for conditions of column water vapor amounts greater than approximately 2.5 cm.

c. *Properties of surface reflectance near 1 μm*

In order to derive information on atmospheric water vapor from satellite measurements of solar radiation reflected by land surface, the surface reflectance properties must be taken into consideration. Most land is covered by either soils, rocks, vegetation, snow, or ice. Figure 2 shows reflectance curves of five major types of soil (Condit 1970; Stoner and Baumgardner 1980). The reflectance over the 0.94-pm water vapor band absorption region change approximately linearly with wavelength. Similar linearity is observed in reflectance spectra of common rocks and minerals. l-he largest deviation from linearity is observed in reflectance spectra of iron-rich soils and minerals. These materials have broad electronic bands, which are related to Fe^{3+} transition and are centered near 0.86 μm. Curve 3 in Fig. 2 shows such a broadband feature in the spectral region between approximately 0.8 and 1.25 μm.

Figure 3 shows vegetation and snow reflectance spectra. These were obtained from surface reflectance spectra compiled by Bowker et al. (1985), and correspond to their number 6 I and number 144 spectra, respectively. The vegetation spectrum has a liquid water band centered at approximately 0.98 pm. The snow spectrum has an ice absorption band centered approximately at 1.04 μm. For comparison, Fig. 3 also shows a calculated water vapor transmittance spectrum. The positions of water vapor, liquid water, and ice absorption bands are relatively shifted. The shifting of the vibrational bands is due to increases in intermolecular forces as the water molecules become more organized in the liquid and solid states (Bunting and d'Entremont 1982).

d) *Instrument characteristics*

Under the vacuum environment in space, the bandpasses of interference filters may change gradually. The bandpasses tend to be shifted or broadened toward longer wavelengths (P. N. Slater 1989, private communication). The shifts can result in changes in mean atmospheric transmission properties over the bandpasses, and therefore affect retrievals of column water vapor amounts from near-l R radiance measurements.

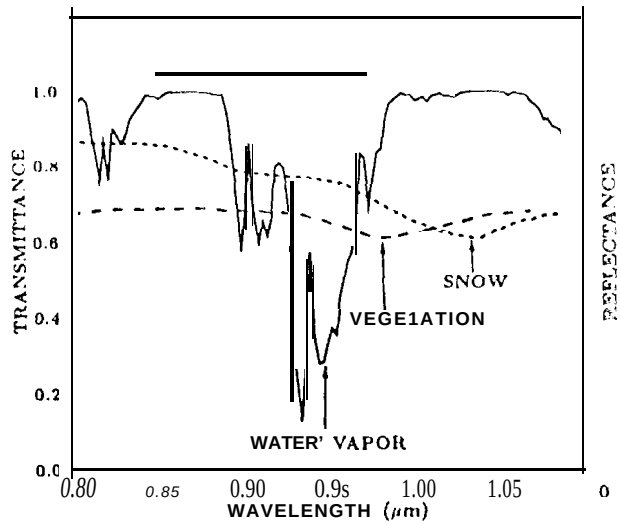

FIG. 3. Examples of a calculated water vapor transmittance spectrum and measured reflectance spectra of vegetation and snow. The water vapor transmittance spectrum is the same as the spectrum in Fig, I with column water vapor amount of 1.2 cm. The vegetation and snow reflectance spectra are obtained from Bowker et al. (1985) and correspond to their number 6 land number 144 spectra, respectively. The band centers of water vapor (-0.94 μm), liquid water ('0.98 μm), and ice (-1.04 μm) are relatively shifted. The bandpasses of the proposed lwo window channels centered at 0.865 and 1.04 μm and one water vapor absorption channel centered at 0.935 μm are also marked with thick horizontal lines.

The changes in bandpasses are usually not monitored on satellites. Recent laboratory studies showed that the bandpasses of some interference filters did not change in the vacuum environment (Y. J. Kaufman 1992, private communication).

e) *Channel selection*

The previous four sections can be summarized as follows. For a satellite measuring solar radiation reflected by land surface targets near 1 pm, $L_{direct}(\lambda)$ is usually 90% of $L_{sensor}(\lambda)$ and $L_{path}(\lambda)$ is typically 10% of $L_{sensor}(\lambda)$. Under the conditions of low aerosol concentrations, the $L_{path}(\lambda)$ can be treated approximately as a fraction of direct reflected solar radiation. Within the 0.94-μm water vapor band absorption region, the 0.935-μm subregion is most sensitive to water vapor changes in dry conditions, and regions near the two edges of the 0.94-μm water vapor band are more sensitive to water vapor changes in moist conditions. The window regions near *0.865* and 1.04 μm have little atmospheric gaseous absorption. The reflectance of many surface targets in and around the 0.94-μm water vapor band absorption region are approximately linear functions of wavelength, although deviations from linearity are obvious for iron-rich soils and minerals, vegetation, and snow. The bandpasses of filters on a satellite instrument may change with time. These factors need to be considered in the channel selection process.

Based on the assumption of linear surface reflectances and on the assumption that the path radiance can be treated as a fraction of direct reflected solar radiation. it can be seen that if a satellite has three near-l R channels, one absorption channel within the 0.94-μm water vapor band absorption region. one window channel near 0.865 Pm. and another window channel near 1.04 μm, then a ratio of apparent reflectance of the absorption channel with a proper combination of apparent reflectance of the two window channels removes the surface reflectance effects, and gives the mean water vapor transmittance of the absorption channel on the sun-surface sensor ray path.

In the channel selection process, we have assumed that the bandpasses of channels may drift to longer wavelengths by O-5 nm. We have required that a 5-nm shift in bandpasses of the selected channels must cause relatively small errors in column water vapor derivations. The bandpasses of our selected absorption channel and window channels are shown in Figs. 1 and 3.1 he selected two window channels are centered at 0.865 and 1.04 μm, respectively, and have the same bandpass of 30 nm. This selection ensures that after shifting the bandpasses of the two window channels to longer wavelengths by 5 nm the bandpasses of both channels will remain in the atmospheric window regions. The selected water vapor channel is centered at 0.935 μm with a width of80 nr^n. Thé mean transmittance over the bandpass of the water vapor channel is also relatively insensitive to a 5-rim shift in the bandpass to longer wavelengths. This is because after the bandpass shifting the decrease in transmittance near the left side of the bandpass of the channel is somewhat compensated by the increase in transmittance near the right side of the bandpass of the channel. The reasons for selecting a broad absorption channel are as follows. The broad channel allows more energy to be collected at geostationary altitude than a narrower channel. The broad channel contains the center portions of the 0.94-μm water vapor band, which are very sensitive to water vapor changes under dry conditions, and the edge portions of the water vapor band, which are sensitive to water vapor changes under moist conditions. As a result, the single broad channel has sensitivity to water vapor changes under both the dry and moist conditions.

A three-channel ratio computed from satellite-measured radiances based on the equation

$$\mathrm{RATIO}_{obs} = \frac{R^*(0.935\ \mu\mathrm{m})}{C_1 R^*(0.865\ \mu\mathrm{m}) + C_2 R^*(1.04\ \mu\mathrm{m})} \qquad (2)$$

is approximately equal to the mean water vapor transmittance over the bandpass of the absorption channel. In Eq. (2), the constant Cl is equal to 0.6, and C_2 0.4. The two constants are determined from the center positions of the three channels. The column water vapor amounts can be obtained from the three-channel ratios using, for example, the method described in section 5.

f. Signal- 1o-noise estimation

The estimates of signal to noise ratios of the three proposed near-IR channels are based on the parameters of GOES1-M series satellites (Rao et al. 1990). Assumptions used in the estimates include: satellite altitude of 35800 km: solar zenith angle of 60°; observational zenith angle of 45"; mean surface reflectance of 0.3; mean surface to sensor transmittances of 0.9 for the two window channels and of 0.5 for the water vapor absorption channel; silicon detectors for the window channel at 0.865 μm and for the absorption channel at 0.935 μm; germanium detector for the window channel at 1.04 μm; optical efficiency of 0.2, that is 20?0 of the energy arriving at the front of the optical system will reach the detectors and detector integration time of O. 1 s. The solar and observational zenith angles are relative to the local vertical direction of the surface area being viewed, instead of relative to the position of the satellite. The local zenith angles determine the total length of sun-surface satellite ray path in the atmosphere. Table I gives estimated signal to noise ratios for the three proposed near-IR channels for 2 X 2. 4 x 4, and 10 x 10 km^2 of the ground instantaneous field of view (GIFOV). The corresponding signal to noise ratios of the three-channel ratio are 250, 1000, and 6250, respectively.

TABLE 1. Estimated signal-to-noise ratios for the three proposed near-IR channels.

Channel center position (gin)	S/N for GIFOV		
	2 X 2 km²	4 X 4 km²	10 X 10 km*
0.865	600	2400	15000
0.935	275	1 100	6.8-IS
I .040	600	2400	15000

4. Sensitivity and error analysis

We evaluate errors in column water vapor derivations from radiances of the three proposed near-IR channels due to 1) finite signal to noise ratio of satellite radiance measurements. 2) nonlinear surface reflectances near I μm, and 3) drifts of satellite channel positions by 5 nm.

a. Sensitivity of three channel ratio

Figure 4 shows the calculated three-channel ratio

$$\text{RATIO}_{\text{cal}} = \frac{T_{\text{mean}}(0.935\ \mu\text{m})}{C_1 T_{\text{mean}}(0.865\ \mu\text{m}) + C_2 T_{\text{mean}}(1.04\ \mu\text{m})} \quad (3)$$

as a function of column water vapor amount using atmospheric and spectral models. In Eq. (3), T_{mean}(0.935 μm) is the mean transmittance over the bandpass of the absorption channel, T_{mean}(0.865 μm) and T_{mean}(1.04 μm) are the mean transmittances over the bandpasses of the two window channels, respectively. Figure 5a, which is obtained from the three-channel ratio sensitivity curve in Fig. 4. shows absolute column water vapor errors for a 1% error in the three-channel ratio under conditions of column water vapor amounts in the 0.5-5-cm range. Figure 5b shows the relative column water vapor error as a function of column water vapor amount. Although the absolute column water vapor error in Fig. 5a increases as the column water vapor amount increases, the opposite is true for the relative column water vapor error in Fig. 5b. It is seen from Fig. 5b that for medium conditions with column water vapor amount in the 2. O-2.5-cm range, a 1% error in the three-channel ratio causes an error of approximately 2.5% in the derived column water vapor amount. This relationship is used in our column water vapor error analysis later.

b. Errors due to finite signal 10 noise ratios

Based on the signal to noise ratios given in Table I and the sensitivity analysis above, errors in column water vapor derivations are estimated to be approximately 1%, 0.25%, and 0.04% for pixel sizes of 2 X 2, 4 X 4, and 10 x 10 km², respectively. For the pixel size of 10 X 40 km² of GOES I-M series satellites. the error in derived column water vapor amounts due to finite signal to noise ratios of the three proposed near-IR channels is negligible.

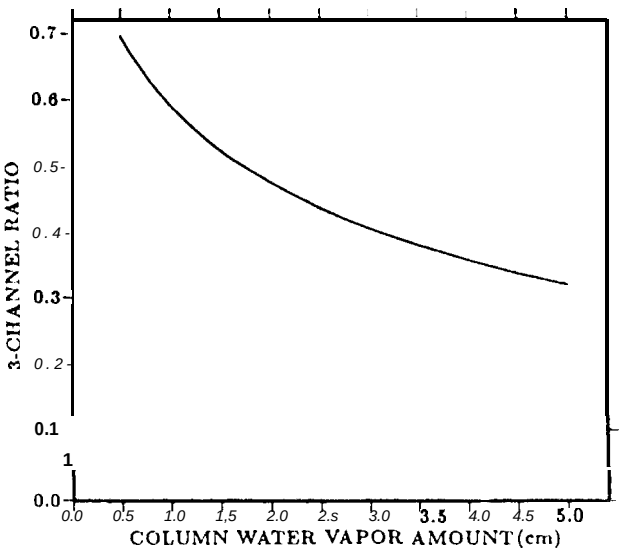

FIG. 4. The dependence of three-channel ratios on the column water vapor amounts. The calculations were made for a solar zenith angle of 60° and an observational zenith angle of 45°.

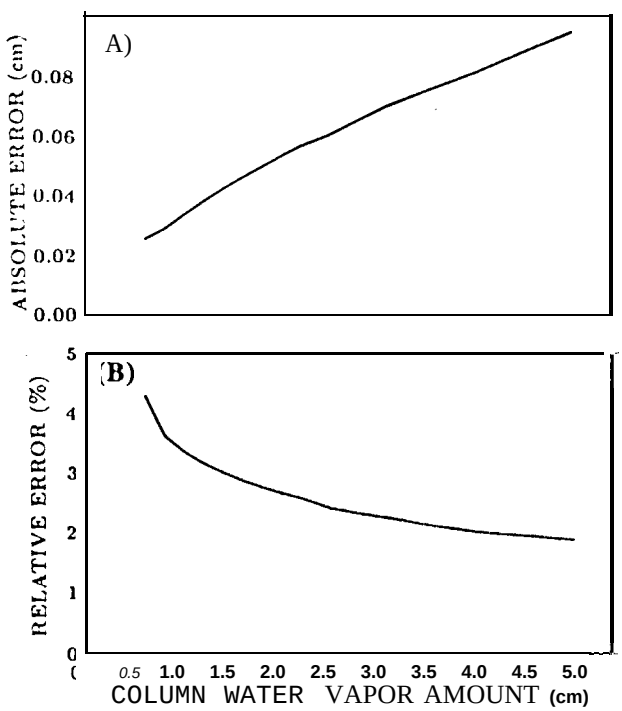

FIG. 5. Absolute column water vapor errors in units of cm for a 1% error in the three-channel ratios under (a) different atmospheric water vapor conditions (a) and (b) the corresponding relative column water vapor errors (b).

c. Errors due to nonlinearity of surface reflectances near 1 μm

A major source of error in deriving column water vapor amounts from measurements of reflected solar radiation by land surface targets is the assumption of linear surface reflectance near 1 μm. This source of error is analyzed in detail below. A total of 155 reflectance spectra of a variety of surface targets were compiled by Bowker et al. (1985). These spectra provide a basis for studying the linearities of reflectance of different surface targets near 1 μm. The spectra were obtained from approximately 60 sources. The quality of the spectra vary significantly; some of the spectra have obvious errors, such as anomalous increases or decreases in reflectance over a very short wavelength interval due to errors in instrument gain factors. Some of the spectra have errors of greater than 20 nm in wavelength calibrations. Some cover a spectral region between approximately 0.4 and 1.0 μm, which is too short for the analysis of linearity of reflectance in the 0.85-1.055-μm region. After eliminating poor-quality spectra by visual inspection, which is somewhat subjective, and eliminating those that do not have sufficient wavelength coverages, a total of 78 reflectance spectra of dry vegetation, green vegetation, minerals and soils, and snow are selected for our analysis.

For each of the selected spectra, the means of reflectances over the bandpasses of the two window channels and the absorption channel are calculated. These mean reflectances are represented by R_{mean}(0.865 μm), R_{mean}(1.04 μm), and R_{mean}(0.935 μm), respectively. A predicted mean reflectance over the bandpass of the absorption channel. $R_{pred.mean}$(0.935 μm), is obtained from R_{mean}(0.865 μm) and R_{mean}(1.04 μm) based on linear interpolation. Then the reflectance error, REFERR, between R_{mean}(0.935 μm) and $R_{pred.mean}$(0.935 μm) is calculated according to

$$\text{REFERR} = \frac{R_{mean}(0.935\ \mu m) - R_{pred.mean}(0.935\ \mu m)}{R_{mean}(0.935\ \mu m)} \quad (4)$$

REFERR is a direct measure of deviations from linearit y of surface reflectance. Figure 6 shows reflectance errors for the 78 selected reflectance spectra, with the horizontal axis representing the spectral number of Bowker et al. (1985). Different symbols are used in the plot to represent different classes of surface targets. Some types of surfaces, such as minerals and soils, have positive and negative reflectance errors. The average reflectance error for a class is calculated using the magnitude of reflectance errors of the spectra in the class.. Table 2 gives the average reflectance errors for different types of surfaces and the corresponding errors in deriving column water vapor values if linear surface reflectances are assumed. Because deviation from linearity is greatest for iron-rich soils, we have separated them from the general mineral and soil class and treated them as another class. Table 2 shows that if surface reflectances are assumed to be linear functions of wavelength when deriving column water vapor values over dry vegetation. green vegetation, mineral and soils. and snow. the systematic errors in the derived column water vapor values are generally less than 5%. For the iron-rich soils, the systematic water vapor error is approximately 8.4%.

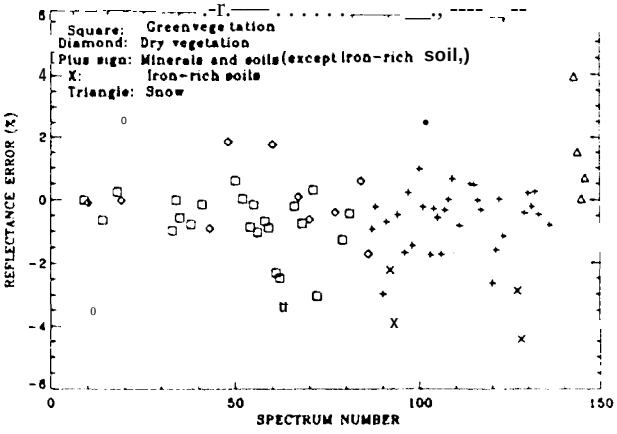

FIG. 6. Reflectance errors defined in Eq. (4) for 78 reflectance spectra compiled by Bowker et al. (1985). The horizontal axis represents the spectral number of Bowker et al. ([985). Different symbols are used for different types of surface targets.

TABLE 2. Average reflectance errors for different surface types and the corresponding systematic errors in derived column water vapor amounts if linear surface reflectances are assumed.

Surface type .	Number of spectra	Reflectance error	Column vapor error
Green vegetation	25	1.0390	2.6%
Dry vegetation	11	0.9790	2.4%
Minerals and soils (except iron-rich soils)	34	1.04'%	2.6%
Iron-rich soils	4	3.36%	8.4%
Snow	4	I.54%	3.9%

Two specific examples of reflectance errors and their corresponding water vapor errors are presented below. The vegetation spectrum in Fig, 3 shows a relatively deep liquid water vapor absorption feature centered at 0.98 μm, in comparison with other vegetation spectra. used in the analysis above. The reflectance error for this spectrum is −2.3%, and the corresponding error in column water vapor derivation is approximately 5.8%. The snow reflectance spectrum in Fig. 3 has an ice absorption feature at 1.04 μm. The reflectance error for this spectrum is 1.5%, and the corresponding error in column water vapor derivation is approximately 4.0%. These two examples show that even if there are liquid and ice absorption features in the 0.85- and 1.055-pm spectral region, the effects of deviation from linearity of surface reflectance are still relatively small.

d. *Errors due to bandpass shifts*

The bandpass shifts discussed previously are usually not monitored on satellites. Our analysis shows that approximately 0.6% of error in the derived column water vapor values will occur when the bandpasses of the two selected window channels are shifted by 5 nm to longer wavelengths while the original unshifted bandpasses are assumed in the column water vapor derivation. The same analysis has been done for the selected water vapor channel. The result shows that a S-rim shift in the bandpass causes an error of 2.5% in the derived column water vapor value.

5. Column water vapor derivation from AVIRIS data

In order to demonstrate the possibility of remote sensing of column water vapor from a geostationary satellite with the proposed three near-IR channels, column water vapor images have been derived from spectral data collected by the Airborne Visible–Infrared imaging Spectrometer (AVIRIS) (Vane 1987) using the three-channel ratioing technique. AVIRIS is currently an operational imaging spectrometer. This instrument images the earth's surface in 224 spectral channels, each approximately IO nm wide, covering the region 0.4–2.5 μm from an ER-2 aircraft at an altitude of 20 km; the pixel size on the ground is approximately 20 X 20 m^2. The AVIRIS data measured over Rogers Dry Lake, California. on 3 I August 1988, and on 23 July 1990 were used in our water vapor retrievals.

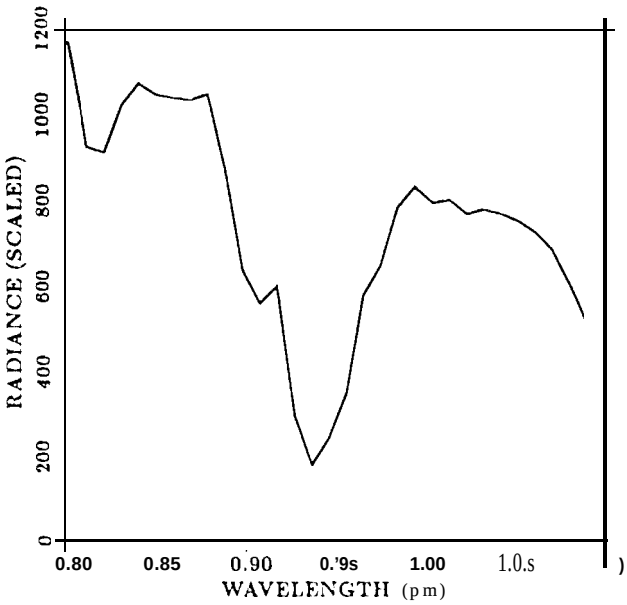

FIG. 8. An AVIRIS spectrum measured on 31 August 1988 in the 0.8–1.1-μm range.

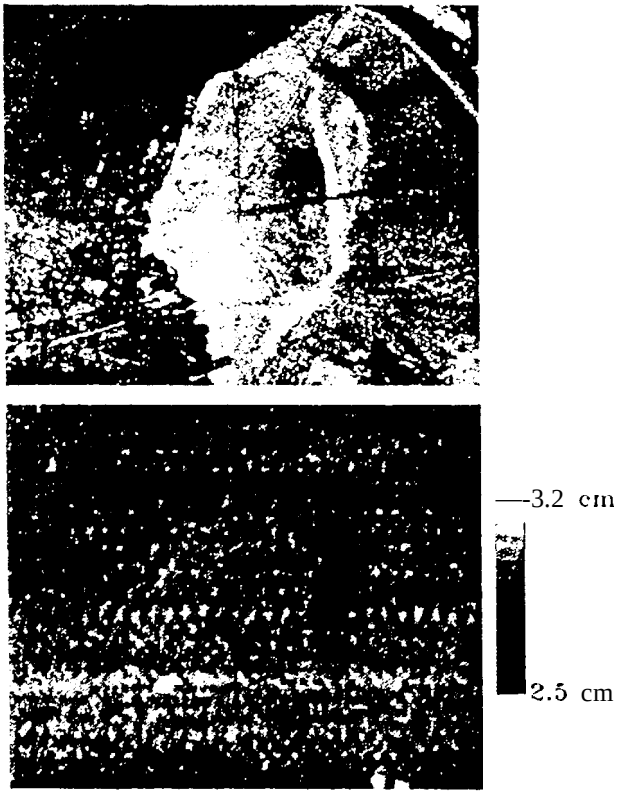

FIG. 7. A 0,865-Pm AVIRIS image (a) of Rogers Dry Lake, California. and the column water vapor image (b) derived from the AVIRIS data using a three-channel ratioing technique. The AVIRIS data were measured on 3 I August 1988.

Rogers Dry Lake. one of the space shuttle landing sites. is located approximately at 35.8" N, I 17.8° W. 1 he surface elevation is about 0.9 km. The 3 I August 1988 AVIRIS data were measured under clear and stable airmass conditions. The upper part of Fig. 7 shows a 0.86-μm image of Rogers Dry Lake. which covers a surface area of approximately 12 X 10 km^2. The brightness varies significantly over the scene because of reflectance differences of the surface targets. The variation of surface elevation within the scene is less than 50 m. Figure 8 shows an AVIRIS spectrum in the 0.8- 1.1 -μm region over a single pixel. The signal-to-noise ratios of the AVIRIS data in the region are approximately 50. There are approximately 20 spectral points in the 0.94-pm water vapor band absorption region and the nearby atmospheric windows. In order to improve the signal to noise ratios, AVIRIS spectra were averaged on a 4-pixel X 4-pixel basis. The spatial averaging increases the signal to noise ratios by a factor of 4 and increases the pixel size to 80 X 80 m^2. The averaged data were divided by the above solar radiance curve to obtain the apparent reflectance.

In order to simulate the three broader channels proposed for remote sensing of column water vapor from future geostationary satellites, apparent reflectance of several AVIRIS channels were averaged to simulate

one broader channel. Specifically, three AVIRIS channels centered at 0.855, 0.865, and 0.875 μm were averaged to simulate one broad window channel with a bandpass between 0.850 and 0.880 μm, three AVIRIS channels centered at 1.028, 1.038, and 1.047 μm were averaged to simulate another broad window channel with a bandpass between 1.023 and 1.052 μm, nine AVIRIS channels within the water vapor absorption region were averaged to simulate one broad absorption channel with a bandpass between 0.899 and 0.985 μm. A three-channel ratio $RATIO_{obs}$ was computed from the apparent reflectance of the broad channels based on Eq. (2). A number of spectra at AVIRIS spectral resolution were calculated using the Malkmus (1967) narrowband spectral model and using atmospheric temperature, pressure, and water vapor vertical distribution profiles measured with a National Weather Service radiosonde released one hour before the AVIRIS overflight but with the column water vapor amounts being scaled by appropriate factors. Three-channel ratios RAI'lOC,I were obtained from the simulated spectra. A table of three channel ratios as a function of column water vapor amount was produced. The column water vapor amount was obtained from $RATIO_{obs}$ using a lookup table procedure. The lower part of Fig. 7 shows a black-and-white image processed from the derived column water vapor values using the three-channel ratioing technique. The image is coded so that black corresponds to a column water vapor of 2.5 cm, and white 3.2 cm. Except for three bright spots, the image is fairly uniform. The dry lake bed is hardly seen in the image. This indicates that the surface reflectance effects are mostly removed in the water vapor retrieval process. The mean of the column water vapor values over the entire scene is 2.87 cm, approximately 2.5% greater than the value of 2.80 cm measured with the radiosonde. 'I he standard deviation of the derived column water vapor values is 3.3%. The standard deviation mainly results from the combination of the finite signal to noise ratios of the AVIRIS data and the differences in nonlinearity of reflectances of surface targets within the scene.

Column water vapor amounts were also retrieved from four sets of AVIRIS data measured at 1852, 1903, 1916, and 1927 UTC 23 July 1990 using the three-channel ratioing technique described above. Although the sky was clear when the AVIRIS measurements were made, there was a weak frontal system passing the site. The upper row from left to right of Fig. 9 shows images processed from radiances of the 0.865-μm channel measured at the four times, respectively. Each of the images covers a surface area of approximately 12 X 12 km^2. The lower row from left to right of Fig. 9 shows the corresponding column water vapor images. l-he images are color coded so that blue corresponds to a column water vapor of 1.95 cm, and red 2.45 cm. These water vapor images showed that drier air intruded into the Rogers Dry Lake area at the later time. An NWS radiosonde released from a place near the lower-left corner of the top-left image 23 minutes prior to the first AVIRIS overflight gave a column water vapor amount of 2.2 cm. Figure 10 shows a time series of column water vapor amounts measured from ground at Rogers Dry Lake with a sunphotometer on the same day. The decreasing of column water vapor amount during the AVIRIS consecutive overflights are seen from this figure.

6. Comparison between reflectance and IR emission techniques

The water vapor profile retrievals from IR emission measurements in the 6- 14-pm region are very sensitive to the assumed surface temperature, atmospheric temperature, and water vapor vertical distributions (Reuter et al. 1988; Hayden 1988). However, retrievals of column water vapor amounts from measurements of solar-radiation reflected by the surface near 1 μm are relatively insensitive to the assumed atmospheric models (Gao and Goetz 1990: Gao et al. 1992). Errors in surface temperatures do not affect water vapor retrievals using the reflectance technique, because the radiation emitted by the surface near I μm is negligible compared to the solar radiation reflected by the surface. The relative insensitivity of retrievals to the assumed temperature profiles from measurements of reflected solar radiation can be explained using the theory of infrared spectroscopy (Goody and Yung 1989). Over the 0.94 μm water vapor band absorption region, there are numerous vibrational-rotational lines. Some of the lines have positive sensitivity to temperature changes. and the converse is true for the other lines. The average effect of all lines in the band has little temperature sensitivity. The relative insensitivity to the assumed water vapor profiles is understandable from the fact that the water vapor value is essentially derived from the mean transmittance of the absorption channel and that the mean transmittance is not very sensitive to the water vapor vertical distributions except, to some extent. pressure.

The proposed reflectance technique works only over land areas (excluding lakes and rivers) during the daytime, while the IR emission technique works over both land and ocean during the day and night. Both the reflectance technique and the IR emission technique provide some information on water vapor above cloud tops. Because the near-IR radiation and the IR radiation do not pass through water clouds, both the reflectance technique and the IR emission techniques fail to provide water vapor information below water clouds. Since the scattered radiation by aerosols also contains water vapor absorption signatures, the reflectance technique may also yield some information on water vapor over the ocean and over lakes and rivers, provided that the signal to noise ratios of radiances from the three near-l R channels are sufficiently high and

FIG. 9. Four 0.865-pm AVIRIS images (upper row) over Rogers Dry Lake, California, and the corresponding four column water vapor images derived from the AVIRIS data. The four sets of AVIRIS data were measured at UTC time of 1852, 1903, 1916, and 1927 UTC 23 July 1990. The water vapor images are color ceded so that blue corresponds to a column water vapor of 1.95 cm, and red 2.45 cm.

that the atmospheric multiple scattering and absorption processes can be modeled properly.

7. Discussion

Near 1 μm, the reflectance of iron-rich soils deviate significantly from linearity. If linearity of reflectance is assumed when deriving column water vapor amounts from radiances of the three near-IR channels measured over these targets, systematic errors of approximately 8% can be introduced. The systematic errors can be reduced if the nonlinearity of reflectances of these targets is taken into account when deriving the column water vapor values. A geologic map of iron-rich soils at an appropriate spatial resolution would be useful when developing operational algorithms for column water vapor amount retrievals from the near-1 R radiance measurements. Because surface reflectance usually change much slower with time than the atmospheric water vapor, the determination of temporal variations of column water vapor amounts using the reflectance technique is expected to be reliable, even if systematic errors are present in the derived column water vapor amounts.

The atmospheric transmission model can be applied to derive column water vapor amounts from measurements of solar radiation near I μm reflected by the surface under low aerosol concentration conditions, that is, with risibilities of 20 km or greater. However, when atmospheric aerosol concentrations are high, scattering effects are important. Scattering effects must be modeled properly when deriving column water vapor amounts from measurements made under hazy conditions.

The bandpasses of interference filters on a satellite instrument must be made as stable as possible. If, for example, the bandpasses of the two window channels are shifted to longer wavelength by more than 10 nm, then the two window channels will be sensitive to water vapor changes, and the three-channel ratio calculated using Eq. (2) will be less sensitive.

The success of column water vapor retrievals (Gao and Goetz [990) from the AVIRIS data has influenced the selection of near-l R water vapor channels (Kaufman and Gao1992) for the Moderate Resolution Imaging Spectrometer (MODIS) (Salomonson et al.

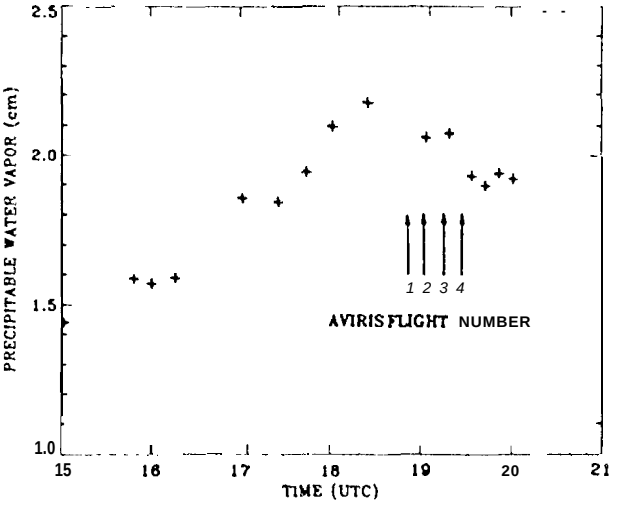

FIG. 10. Time series of precipitable water vapor measured with a sunphotometer over Rogers Dry Lake, California, on 23 July 1990.

1989), a polar-orbit satellite instrument currently scheduled for launching in 1998. MODIS will have three water vapor sensitive channels within the 0.94-μm water vapor band absorption region, instead of the one broad water vapor absorption channel proposed in this paper.

8. Summary

Three near-IR channels, one water vapor absorption channel centered at 0.935 μm with a width of 80 nm, and two window channels centered at 0.865 and 1.04 μm, respectively, with the same width of 30 nm, are proposed for remote sensing water vapor over land areas during daytime from future geostationary satellite platforms. The three-channel ratio, calculated according to Eq. (2), removes the effect of linear variations of surface reflectance with wavelength and gives approximately the mean water vapor transmittance of the absorption channel. The column water vapor is derived from the three-channel ratio. The signal-to-noise ratios of radiances from the three near-IR channels at GIFOV of 2×2 km^2 are sufficiently high to produce column water vapor values at a precision of approximately 1%. Systematic errors in derived column water vapor values by assuming that the surface reflectance changes linearly with wavelengths are typically 5% or less, except for the derivation over areas covered by iron-rich soils. Retrievals of column water vapor amounts from the AVIRIS data at a precision better than 5% have been made. Temporal variations of column water vapor amounts by less than O. 1 cm have been determined from the AVIRIS data. The proposed near-IR reflectance technique for remote sensing water vapor from future geostationary satellite platforms is expected to yield column water vapor amounts with much higher precision than using the IR emission techniques, and to complement water vapor measurements using the IR emission techniques in the boundary layer where most of the water vapor is located.

Acknowledgments. The authors are grateful to K. Heidebrecht at the Center for the Study of Earth from Space, University of Colorado at Boulder for helpful comments on the manuscript. This work was partially supported by the NASA/Goddard Space Flight Center under contract NAS5-30552.

REFERENCES

Bird. R.E., and R. Hustrom, 1982: Precipitable water measurements with sun photometers, *J. Appl. Meteor.*, 11 96– 1201.

Bowker, D.E., R, E.Davis, D.L.Myrick, K. Stacy, and W. T. Jones. 1985: Spectral reflectances of natural targets for use in remote sensing studies, *NASA Ref. Publ. 1139.*

Bunting, J. I".. and R. P. d'Entremont, 1982: Improved cloud detection utilizing defense meteorological satellite program near infrared measurements. AFGL-TR-82-0027, Air Force Geophysics Laboratory, Bedford. Mass., IO- 11.

Chesters, D. C.. L. W. Uccellini, and W. D. Robinson, 1983: Low-level water vapor fields from the VISSR Atmospheric Sounder (VAS) "split-window'" channels, *J. Climate Appl. Meteor.*, 22, 725-743.

Condit, H. R., 1970: The spectral reflectance of American soils. *Photogramm. Eng.*, *36, 955-965.*

Esaias, W., et al.. 1986: Moderate resolution imaging spectrometer. *Earth Observing System*, vol IIb, *Instrument Panel Report*, NASA, Washington, D.C., 49-53.

Fowle, F. E., 1912: The spectroscopic determination of aqueous vapor. *Astrophys. J.*, *35, 149-162.*

Frouin, R., P.-Y. Deschamps, and P. Lecomte, 1990: Determination from space of atmospheric total water vapor amounts by differential absorption near 940 nm: Theory and airborne verification, *J. Appl. Meteor.*, 29, 448-460.

Gao, B. C., and Alexander F. H. Goetz, 1990: Column atmospheric water vapor and vegetation liquid water retrievals from airborne imaging Spectrometer data. *J. Geophys. Res.*, 95, 3549-3564.

-----, Ed. R. Westwater, B. Boba Stankov, D. Birkenheuer, and Alexander F. H. Goetz, 1992: Comparison of column water vapor measurements using downward-looking optical and infrared imaging spectrometry and upward-looking microwave radiometry, *J. Appl. Meteor.*, 1 193-1201.

Goody, R. M.. and Y. L. Yung, 1989: *Atmospheric Radiation.* Oxford Univ. Press, 519 pp.

Hayden, C. M.. 1988: GOES-VAS simultaneous temperature-moisture retrieval algorithm. *J. Appl. Meteor.*, 27, 705-733.

Iqbal, M.. 1983: *An Introduction to Solar Radiation.* Academic, 43-95.

Kaufman. Y. J., and B.-C, Gao. 1992: Remote sensing of water vapor in the near 1 R from EOS/ MODIS. *IEEE Trans. Geosci. Remote. Sensing, 30.87* 1 -884.

Kneizys, F. X.. E. P. Shettle, W. O. Gallery, J. H. Chetwynd, L. W. Abreu, J. E. A. Selby, S. A. Clough, and R, W. Fenn, 1983: Atmospheric transmittance/radiance: Computer code LOWTRAN-6. *AFGL-TR-83-0187.* Air Force Geophys. Lab.. Bedford. Mass.

Malkmus, W.. 1967: Random Lorentz band model with exponential-tailed S line intensity distribution function. *J. Opt. Soc. Am.*, 57.323-329.

Rae. P. K., S. J. Holmes, R. K. Anderson. J. S. Winston, and P. E. Lehr. 1990: *Weather Satellites. Systems, Data and Environmental Applications* American Meteorological Society. Boston. 55-59.

Reuter, D.. J. Susskind, and A. Pursch, 1988: First-guess dependence of a physically based set of temperature-humidity retrievals from HIRS2/ MSU data, *J. Atmos. Oceanic. Technol.*, 5, 70-83.

Salomonson, V. V., W. L. Barnes. P. W. Maymon. H. E. Montgomery, and H. Ostrow, 1989: MODES: Advanced facility instrument for studies of the earth as a system. *IEEE Trans. Geos. Remote Sens.*, 27.145-153.

Starr. D. O'C.. and S. H. Melfi, 1991: The role of water vapor in climate, A strategic research plan for the proposed GEWEX water vapor project (GVap), NASA Conf. Publ. 3120. 50 pp.

Stoner, E.R., and M. F. Baumgardner, 1980: Physiochemical, site and bidirectional reflectance factor characteristics of uniformly moist soils, 1-50, NASA CR-16057 1.

Susskind, J., J. Rosenfield, and D. Reuter, 1984: Remote sensing of weather and climate parameters from HIRS2 / MSU on TIROS-N. *J. Geophys. Rev.*. 89,4677-4697.

Vane, G.. Ed., 1987: Airborne visible/infrared imaging spectrometer (A VIRIS), JPL Publ. 87-38. Jet Propul. Lab,. Pasadena. Calif., 3-97.

Voltz, F, E., 1974: Economic multispectral sun photometer for measurements of aerosol extinction from 0.44 μm to 1.6 μm and precipitable water. *Appl. Opt.*, 13.1732-1733.